Nuclear Inst. and Methods in Physics Research, A 1051 (2023) 168212

Contents lists available at ScienceDirect

Nuclear Inst. and Methods in Physics Research, A

journal homepage: www.elsevier.com/locate/nima

Full Length Article

New method for unfolding neutron source spectra

Victor Pérez-Medina-Ollivary *, Armando Varela-González, Jaime Klapp, Rafael Policromeades-Rueda

Instituto Nacional de Investigaciones Nucleares (ININ), Carretera México Toluca S/N, La Marqueza, Ocoyoacac, 52750 Estado de México, Mexico

ARTICLE INFO

Keywords:
Neutron unfolding
Neutron spectroscopy
Bonner spheres
Neutron detectors

ABSTRACT

For solving the Fredholm equation of the first kind, the domain can be discretized in M spheres and N energy bins using a Bonner multisphere spectrometer, in which the neutron flux is to be deduced from the response matrix $R_{ij}(E)$, and the count rate obtained for each sphere C_i. For this study we use an approach that introduces certain neutron energy indeterminations, which are difficult to account for if some absolute calculations are required to be performed. For M different from N, a problem arises after obtaining the deconvolution of this equation, because the extracted solution is not unique, even if a host neutron energy spectrum is used. We propose a different method for extracting neutron energy spectra from the count rate obtained using a Bonner spectrometer. The method consists of partitioning the response matrix into a number of matrices such that M is equal to N, and depends on the response matrix and the number of spheres under consideration. Thus, the overall solution of the Fredholm equation can be divided and applied to N/M segments with M equations, and M unknowns, which can be solved in every energy segment for the neutron energy spectra. With this, the neutron spectra can be recovered by combining successive energy intervals as will be thoroughly described in the paper.

1. Introduction

Using a Bonner Sphere Spectrometer (BSS), requires a well-established and validated response function for each sphere, defined as the reading per unit fluence as a function of neutron energy, usually calculated using Monte Carlo (MC) codes, and validated with calibration measurements. The differences between methods with their advantages and disadvantages obtained by measuring and using several methods in situ has been described by Barros [1]. In all of them they approach a given spectrum a priori with a good approximation.

The problem of deriving the neutron spectrum from a set of multisphere neutron spectrometer measurements has no unique solution, and many different spectra are consistent with the data. There are many unfolding computer programs to obtain the energy spectra [2–6] where they use an a priori spectrum in order to find a result which is very usefully if you do not know the spectrum. All the codes discussed in this article approximate the solution to an a priori spectrum, and the resulting spectrum is approximately equal to that sought, in particular, for example, Heydarzade et al. [7], use SAND II which is a code made for unfolded spectra with activation detectors, however, you can use Bonner spheres if you enter the response functions of these spheres. The contribution of each energy group in the spectrum is calculated by the expression, $\varphi^{k+1,}{}_{,j} = \varphi^{k}{}_{,j}\, e^{C^k}$, where k and j are the iteration loop number, and the energy group number, respectively. The parameter C depends on the activity of the target foil in the energy range of the corresponding group. The iteration loop takes place until the amount of final activity computed by the code converges to the experimental activity. As mentioned above, the value of foils activities depends on the geometry of the source and irradiation situation, which cannot be considered in this code. The method approximates the a priori spectrum to the experimental measurements until a sufficiently small error has been reached, or until a maximum number of iterations is reached. It is obvious, that the method can determine an unknown spectrum, but it is necessary to use statistical method to compare the results. The method proposed in this article does not attempt to determine an unknown spectrum, but to determine accurately a known spectrum that has only been modified by the room scattering, and by the errors intrinsic to the construction of the detector.

Existing methods calculate an approximate spectrum, and it is important to estimate the response functions with good accuracy. In addition, the scattering must be corrected and can be estimated for example, using Monte Carlo simulation techniques.

Following our method, with the response functions and the spectrum taken from tables [8,9], a theoretical spectrum is obtained by applying the Fredholm equation of the first kind (Eq. (4)). The theoretical spectrum can be recovered from the inverse matrices, and after

* Corresponding author.
E-mail addresses: victor.medina@inin.gob.mx (V. Pérez-Medina-Ollivary), armando.varela@inin.gob.mx (A. Varela-González), jaime.klapp@inin.gob.mx (J. Klapp), rafael.poli@inin.gob.mx (R. Policromeades-Rueda).

https://doi.org/10.1016/j.nima.2023.168212
Received 12 October 2022; Received in revised form 7 February 2023; Accepted 13 March 2023
Available online 21 March 2023

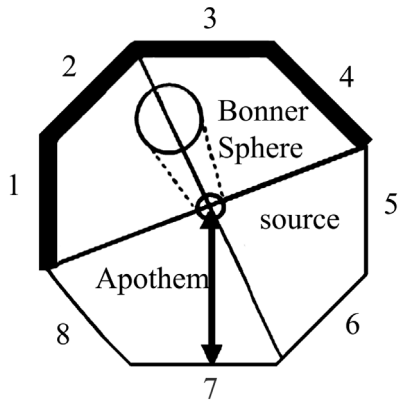

Fig. 1. Octagonal neutron room with an apothema of 4 m, four concrete walls (thick lines 1-4), and four thin sheet walls (thin lines 5-8).

determination of the experimental spectrum, which is proportional to theoretical spectrum.

In the context of this article, numerical simulations are not performed, nor are statistical methods used, we analytically solve MXM square equation systems. In particular, 6×6 and 5×5 equations were solved by $4 \cdot 4$ and $10 \cdot 2$ mm^2 detectors, respectively, and where the determinants of the systems are non-zero, so the solutions are unique and have no uncertainties.

We assume that the method can be good, when used for example, by laboratories that has only one or two sources and is difficult to calculate the response functions of their spheres and since these are adjusted by bombarding the spheres with mono-energetic neutrons.

We use the neutron source ^{241}AmBe(α, n), and the ^{252}Cf fission neutron source. The objective of this work, is to show that when the theoretical measurements calculated with a known spectrum are introduced by solving the Fredholm equation (Eq. (4)), the spectrum is recovered identically, and when the real BSS measurements are introduced, the spectrum is proportional to the theoretical input spectrum, and the differences only occur due to the laboratory design. Measured and calculated fluences and fluence responses of instruments, are known only with finite uncertainty, however, in the context of this work, the fluence responses taken from the compendium [8], are considered uncertainties free, as they only depend on the specific situation of an actual experiment. However, if conclusions are to be drawn on the use of a particular instrumentation, it is necessary to make a variance analysis for the specific situation. In view of this, only three digits are given for numerical values in the compendium [9], and only two are considered to be significant. During certain dose rate neutron dosimeter and/or neutron monitor device calibrations, carried out in the neutron Metrology Laboratory of the National Institute of Nuclear Research (ININ, México), using a calibrated Am–Be and/or Cf neutron sources, we encountered the challenge of the requirement to know the real neutron energy spectra impinging on every Bonner sphere, considering the scattering material surrounding the experimental arrangement. As indicated above, deconvolution methods do not extract unique solutions for the neutron spectra, and introduce uncertainties in the calculus of some parameters, such as the ambient dose equivalent $H^*(10)$, personal dose equivalent H_p (10), and the effective dose equivalent E.

Data were taken at the neutron room of the ININ Metrology Laboratory, using a Bonner spectrometer ($^6LiI(Eu)$), $4 \cdot 4$ mm^2, and $10 \cdot 2$ mm^2, together with six moderating spheres (2, 3, 5, 8, 10, and 12 in diameter), as described elsewhere.

Bonner sphere counting was calibrated with a standard ^{241}AmBe(α, n) neutron source, using the Eisenhauer–Schwartz model [10] for the calibration of spherical detectors, and the efficiencies of the spheres were determined if the calibration factor for the flux (n/s·cm^2) was N_h, and the flow is

$$\varphi(D) = N_h C(D), \tag{1}$$

where C(D) is the reading in n/s at a distance D. Considering $C(D) = 1/N_h$, we obtained the measurements of each sphere for a normalized flow. In our laboratory, the neutron room is octagonal with an apothem of 4 m. Four walls are of made concrete to protect the personnel, and the other four are thin iron sheets oriented to the garden to avoid neutron scattering. The calibration measurements were taken along the symmetry plane of the room. Fig. 1 shows a horizontal sectional view.

Matrix response functions from Griffith et al. (1990) [9] for the small crystal and Hakim et al. [11] for the $10 \cdot 2$ mm^2 crystal were used with the ^{241}AmBe and ^{252}Cf neutron energy spectra, recommended by the International Atomic Energy Agency (AIEA) [9].

Table 1
Theoretical and experimental measurements for the ^{252}Cf neutron source, the room scattering S, and the correction factor f.

D	C^{IAEA}	C^{Exp}	10^5·S(Scattering)	$f=C^{Exp}/C^{IAEA}$
3	1.01E−01	4.96E−02	8.27E+00	4.93E−01
5	2.88E−01	1.71E−01	5.51E+00	5.94E−01
8	3.20E−01	2.20E−01	4.54E+00	6.86E−01
10	2.56E−01	1.78E−01	2.86E+00	6.95E−01
12	1.79E−01	1.55E−01	3.60E+00	8.62E−01

Table 2
Theoretical and experimental measurements for the ^{241}AmBe neutron source, the room scattering S, and the correction factor f.

D	C^{EXP}	C^{IAEA}	S(Scattering)	10^4 S	$f=C^{Exp}/C^{IAEA}$
2	1.10E−02	3.05E−02	2.31E−04	2.31E+00	2.78E+00
3	3.53E−02	7.27E−02	1.01E−04	1.01E+00	2.06E+00
5	1.24E−01	2.41E−01	2.67E−05	2.67E−01	1.95E+00
8	2.01E−01	3.23E−01	1.32E−05	1.32E−01	1.61E+00
10	1.82E−01	2.79E−01	3.23E−05	3.23E−01	1.53E+00
12	1.93E−01	2.13E−01	1.03E−05	1.03E−01	1.10E+00

2. Calibration method

The general functional relationship for the detector reading in open geometry [10], C(D), at the separation distance between the geometric center of the radioactive source and the front face, or surface, of the detector, D, is given by:

$$C(D) = \frac{K F_1(D) F_2(D)}{(D + R_E)^2}. \tag{2}$$

The function $F_1(D)$ is the geometric correction, $F_2(D)$ is the total air and room scattering correction factor, K is the source–detector combination characteristic constant, and R_E is the distance from the front face or surface of the detector to the effective center. Important for this work is $F_2(D)=1+AD_0+SD_0^2$ in order to give the values of room scattering S obtained in the sphere calibration.

Tables 1 and 2 indicates the results for ^{252}Cf and ^{241}AmBe sources, respectively.

3. The new unfolding method

Neutron spectrum unfolding from readings has been described by a system of Fredholm integral equations of the first type [12]. If a neutron Bonner spectrometer is used, the count rate measured by the ith Bonner sphere, C_i, is related to the response function R(E) and the

known energy spectra $\varphi(E)$, wherein the system is exposed through the relation

$$C_i = \int_{E_{min}}^{E_{max}} R(E)\varphi(E)dE, \tag{3}$$

where $i = 1, 2, \ldots, M$ spheres.

To obtain a numerical solution, Eq. (2) is written in terms of a set of discrete equations, as described by the so called Fredholm equation:

$$C_i = \sum_{\rho=1}^{N} R_{ij}\varphi_j, \tag{4}$$

where $R_{ij}(E_j)$ is the response function of the ith sphere to neutrons of energy E_j, N the number of energy bins, and $\varphi(E_j)$ is the fluence of the jth energy bin. As mentioned in the introduction we analytically solve MXM square equation systems.

Considering, Eq. (4) has no unique solution because the system is inconsistent if M is different from N, and M is the number of spheres used, N > M, however, this can be overcome by segmenting the fluence energy interval into N/M groups, giving rise to square matrices of M × M order, which can be solved for each group of the energy spectrum in an ordered and ascending manner. To adjust the number of energy bins according to the number of spheres used, it is necessary to interpolate or omit some energy elements in the response matrix so that M is a multiple of N. Once this step is achieved, according to Eq. (4), and using the initial response matrix and energy spectra stated, it is possible to calculate the ideal or theoretical count rate as the product of $R_{ij}\varphi_j$ values for each sphere i, which are grouped into N/M=G groups.

Rewriting Eq. (4) as N/M Equations, we obtain the following equation:

$$\sum_{\pi=1}^{M} C_i(IAEA) = \sum_{\rho=1}^{M} R_{ij}\varphi_j(IAEA), \sum_{\pi=M+1}^{2M} C_i(IAEA)$$

$$= \sum_{\rho=M+1}^{2M} R_{ij}\varphi_j(IAEA), \ldots, \sum_{\pi=N-M+1}^{N} C_i(IAEA) = \sum_{\rho=N-M+1}^{N} R_{ij}\varphi_j(IAEA). \tag{5}$$

In each N/M equations, we can obtain the inverse of the square matrices R_{ij}. If we define the inverse of the matrix $R_{ij}=(R_{ji})^{-1}$ with the M theoretical values for each segment $C_{1,M}, C_{M+1,2M}, \ldots, C_{N-M+1,N}$, with Eq. (6) and because they were calculated in ascending order for each sphere's diameter, the values for each N/M matrix can be obtained as:

$$\varphi^i(IAEA) = \sum_{j=1}^{M}[(R)^{-1}]_{ji}C_j(IAEA), \quad i = 1, 2, \ldots, M, \tag{6}$$

$$\varphi^i(IAEA) = \sum_{j=M+1}^{2M}[(R)^{-1}]_{ji}C_j(IAEA), \quad i = M+1, 2, \ldots, 2M, \tag{7}$$

$$\varphi^i(IAEA) = \sum_{j=N-M+1}^{N}[(R)^{-1}]_{ji}C_j(IAEA), \quad i = N-M+1, 2, \ldots, N. \tag{8}$$

With a total of N values for φ which must be identical to the original values of the theoretical spectrum taken from the IAEA tables [9].

Taking the theoretical values as a basis, first normalize the $R_{ij}\varphi_j$ for each sphere and then multiply them by the experimental values C_i^{exp}, the new sum for each sphere will be N experimental values (Not M):

$$C_j^{exp} = C_i^{exp} \cdot \frac{R_{ij}\varphi_j}{\sum_{\rho=1}^{N} R_{ij}\varphi_j}, \tag{9}$$

where $i = 1, 2, \ldots, M, j = 1, \ldots, N$.

Sometimes it is necessary to work with the experimental measurements normalized:

$$C_j^{exp}(nor) = \frac{C_i^{exp}}{\sum_{\rho=1}^{M} C_j^{exp}}, \tag{10}$$

Table 3
Calculated values with the values reported in Table 1 for the ^{252}Cf neutron source.

μ_f	μ_S	Covariance
1.84E+00	6.91E−01	0.37
σ_f	σ_S	Regression coefficient
5.21E−01	7.85E−01	0.90

Table 4
Calculated values with the values reported in Table 2 for the ^{241}AmBe neutron source.

μ_f	μ_S	Covariance
1.55E−05	4.96E−05	4.90E−11
σ_f	σ_S	Regression coefficient
2.89E−06	1.88E−05	0.90

and $j = 1, \ldots, M$. To obtain the unfolded spectra for the experimental measurements, a new response functions must be calculated as:

$$(NR_{ij})^{ij} = \frac{C_j^{exp}}{C_j} R_{ij}, \tag{11}$$

where $j = 1, 2, \ldots, M$, and $i = 1, 2, \ldots, N$.

Again, multiplying by φ_j, and applying Fredholm Eq. (4), we obtain that:

$$C_i^{exp} = \sum_{\rho=1}^{N}(NR_{ij})^{ij}\varphi_j. \tag{12}$$

Segmenting again C_j^{exp}, similar equations are calculated, first for Eq. (5) and after for Eq. (6), this is:

$$\sum_{\pi=1}^{M} C_i(exp) = \sum_{\rho=1}^{M}(NR)^{ij}\varphi_j(exp), \sum_{\pi=M+1}^{2M} C_i(exp)$$

$$= \sum_{\rho=M+1}^{2M}(NR)^{ij}\varphi_j(exp), \ldots, \sum_{\pi=N-M+1}^{N} C_i(exp) = \sum_{\rho=N-M+1}^{N}(NR)^{ij}\varphi_j(exp). \tag{13}$$

And similarly, we obtain N/M square equations MxM for the unfolding spectrum of the experimental measurements equivalent to Eqs. (7)–(9):

$$\varphi^i(exp) = \sum_{j=1}^{M}[(NR)^{-1}]^{ji}C_j(exp), \; i = 1, 2, \ldots, M, \tag{14}$$

$$\varphi^i(exp) = \sum_{j=M+1}^{2M}[(NR)^{-1}]^{ji}C_j(exp), \; i = M+1, 2, \ldots, 2M, \tag{15}$$

$$\varphi^i(exp) = \sum_{j=N-M+1}^{N}[(NR)^{-1}]^{ji}C_j(exp), \; i = N-M+1, 2, \ldots, N. \tag{16}$$

4. Results and discussion

As stated above, the uncertainties of the spectra are not reported in the IAEA compendium [9]. An analysis of variance was performed for the correction factor applied to the response function ($f = C^{Exp}/C^{IAEA}$), which has been defined by Eq. (11), and the room scattering S calculated in Eq. (2) by the factor S(D) in the calibration of the spheres. Values for S and f are reported in Tables 1 and 2 for the ^{252}Cf and ^{241}AmBe sources, respectively, together with the theoretical (IAEA) and experimental measures. The average values for, f (μ_f) and S (μ_S) are reported in Tables 3 and 4, for all spheres and their standard deviations are, respectively, σ_f and σ_S. With these the covariance and

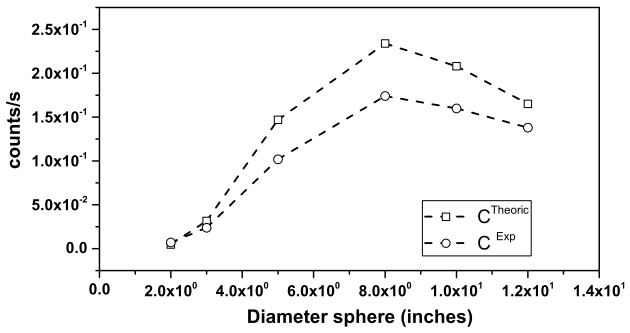

Fig. 2. Theoretical and experimental values taken with the BSS 4×4 $^{6}LiI(Eu)$.

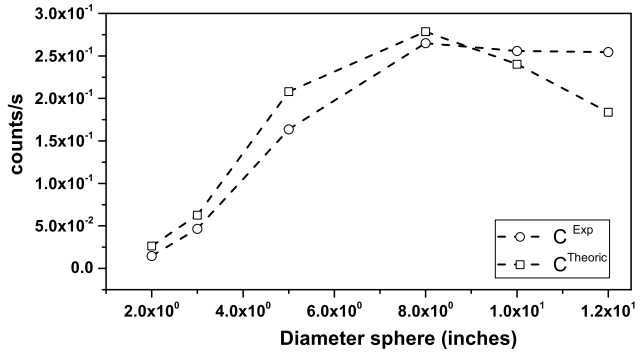

Fig. 3. Theoretical and experimental normalized values taken from Table 1.

the correlation coefficient between the two variables are calculated for the ^{252}Cf source in Table 3, and for the ^{241}AmBe source in Table 4, finding that f and S are strongly correlated with a factor of 0.9. Hence, it follows that corrections made to the response functions, are mainly due to the scattering of neutrons produced by the calibration room, and the resulting spectra are well estimated.

Our method was applied to two neutron sources, ^{241}AmBe and ^{252}Cf, and the measurements were taken using two spectrometers, with $^{6}LiI(Eu)$ crystals of different sizes, $4 \cdot 4$ mm^2 and $10 \cdot 2$ mm^2. The reference spectra and response functions were obtained from the IAEA Compendium Report [9]. In most cases, the measured or computed neutron spectra were originally obtained as group fluences in energy bins. This compendium uses a standard energy grid. Throughout this compendium, the values representing the neutron spectra, as $\Phi_E(E)$ in the tables, are group fluences divided by the lethargy intervals $ln(E_{i+1}/E_i)$ and, consequently, normalized.

Theoretical and experimental measurements of the ^{241}AmBe neutron source obtained using the $4 \cdot 4$ mm^2 crystal are listed where normalized values are also displayed. Fig. 2 shows the unnormalized values, whereas Fig. 3 shows the normalized values.

Fig. 4, shows the spectrum of the ^{241}AmBe neutron source with a $4 \cdot 4$ mm^2 crystal.

Here, $\varphi^{theo}(^{241}\text{AmBe})$ represents the theoretical input spectrum (IAEA), and $\varphi^{nor-exp}(4 \cdot 4)$ represents the experimental normalized measured spectrum with the $4 \cdot 4$ ^{6}LiI crystal.

And as a result, the experimental spectrum obtained with the normalized measurements is proportional to the theoretical spectrum entered in the calculations:

$$\varphi^{nor-exp}(4x4) = 1.653 \cdot \varphi^{theo}(^{241}AmBe). \tag{17}$$

To demonstrate the consistency of the method, two more spectra were obtained, the first using a $^{6}LiI(Eu)$ with a $10 \cdot 2$ mm^2 crystal, and with the response functions of Dr Mazrou [11], and the second with the IAEA response functions, with a Cf^{252} neutron source taken from de Compendium [8].

Fig. 5 show the theoretical and experimental measures of the values in neutrons per second for the $10 \cdot 2$ mm^2 crystal and the ^{241}AmBe source.

The corresponding image of the experimental spectrum taken using a $^{6}LiI(Eu)$ with a $10 \cdot 2$ mm^2 crystal, with the response functions of Dr Mazrou [11], is omitted because it is the same as the IAEA spectrum [9], in this unfolding the measures did not have to be normalized (Eq. (10)).

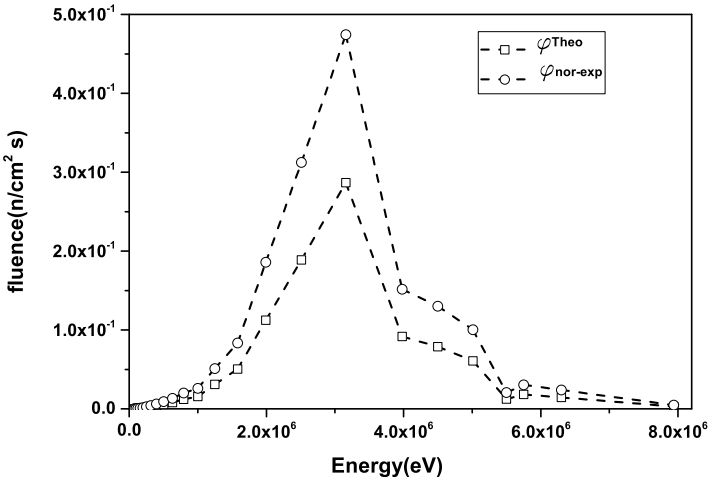

Fig. 4. Theoretical and experimental Spectra (^{241}AmBe Source), $\varphi^{nor-exp}(4 \times 4) = 1.653 \cdot \varphi^{theo}(^{241}\text{AmBe})$.

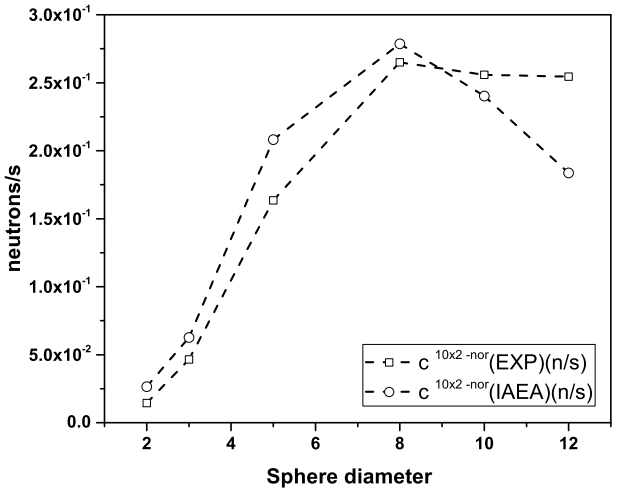

Fig. 5. Theoretical and experimental normalized measurements for ^{241}AmBe.

Table 5
Theoretical, experimental and normalized measurements for ^{252}Cf.

D	$^{252}Cf_i^{nor}(10\cdot 2)$	$^{252}Cf_i^{exp-nor}(10\cdot 2)$	σ
3	8.79E−02	6.42E−2	1.23E−4
5	2.52E−01	6.42E−02	1.23E−04
8	2.80E−01	2.84E−01	4.49E−4
10	2.24E−01	2.30E−01	4.55E−04
12	1.57E−01	2.00E−01	4.88E−04

The other unfolding was for a ^{252}Cf source with the same detector, 10·2 mm^2 crystal, reducing the spectrum to 25 points from 30 published by the IAEA, [8], normalized measurements results are presented in Table 5 and Fig. 6.

Fig. 6 shows the ^{252}Cf spectrum for the normalized measurements obtained with the BSS and normalized theoretical measurements.

where $^{252}Cf^{Exp}$ is the experimental spectrum of ^{252}Cf and $^{252}Cf^{Theo-nor}$ is the theoretical normalized spectrum.

To obtain this spectrum, the measurements were normalized, and the resulting spectrum was proportional to the theoretical spectrum

$$^{252}Cf^{Exp} = 1.14 \cdot ^{252}Cf^{Theo-nor}, \quad (18)$$

Not all spectra were obtained by normalizing the readings, however the three unfolding done were obtained using the calculated new response function NR_{ij} (Eq. (11)).

5. Conclusions

Both, the response functions and spectra are independent of the characteristics of the calibration room and depend only on the energy and not on the neutrons scattered in the room. However, the theoretical values are obtained when a source for the experimental readings is different from a real source and if the reading from the latter are entered directly into the calculations of this work, a spectrum similar to the theoretical input spectrum is not obtained. To obtain a similar spectrum, the response functions were corrected with the factor presented in Eq. (11), which can be justified by the fact that the scattered neutrons change their energy in different laboratories, and it is necessary to correct these functions.

Declaration of competing interest

The authors declare that they have no known competing financial interests or personal relationships that could have appeared to influence the work reported in this paper.

Data availability

Data will be made available on request.

Acknowledgments

We thank H. Mazrou for the response functions provided to us, and Efrain Chávez from the Physics Institute of the National Autonomous University of Mexico (IFUNAM) for useful discussions on the manuscript. We thank ININ for allowing us to conduct this research.

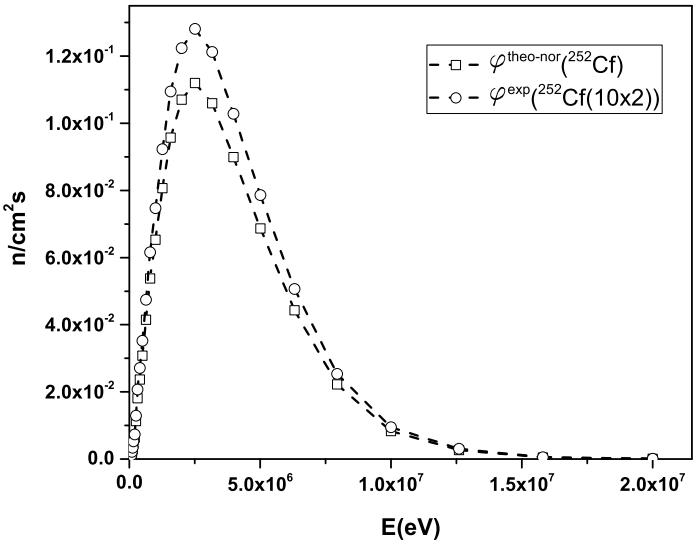

Fig. 6. Theoretical and experimental normalized measurements for ^{252}Cf.

References

[1] S. Barros, V. Mares, R. Bedogni, M. Reginatto, A. Esposito, I.F. Gonçalves, P. Vaz, W. Rühm, Comparison of unfolding codes for neutron spectrometry with Bonner spheres, Radiat. Prot. Dosim. 161 (1–4) (2014) 46–52.

[2] M. Reginatto, P. Goldhagen, N. S., Spectrum unfolding, sensitivity analysis and propagation of uncertainties with the maximum entropy deconvolution code MAXED, Nucl. Instrum. Methods A (2002).

[3] W. McElroy, S. Berg, T. Crockett, R. Hawkins, Spectra Unfolding, Tech. Rep., US Air Force Weapons Laboratory, 1967.

[4] A. Sannikov, BON94 Code for Neutron Spectra Unfolding from Bonner Spectrometer Data, Tech. Rep., CERN/TIS-RP/IR/94-16, 1994.

[5] F. Brooks, H. Klein, Neutron spectrometry—historical review and present status, Nucl. Instrum. Methods Phys. Res. A 476 (1–2) (2002) 1–11.

[6] S. Maeda, H. Tomita, J. Kawarabayashi, T. Iguchi, Fundamental study on neutron spectrum unfolding using maximum entropy and maximum likelihood method, Prog. Nucl. Sci. Technol. 1 (2011) 233–236.

[7] A. Heydarzade, Y. Kasesaz, S. Mohammadi, Coupling the SAND-II and MC-NPX codes for neutron spectrum unfolding, J. Instrum. 13 (08) (2018) P08010.

[8] R.V. Griffith, J. Pálfalvi, U. Madhvanath, Compendium of neutron spectra and detector responses for radiation protection purposes, 1990.

[9] A. AC03347667, Compendium of Neutron Spectra and Detector Responses for Radiation Protection Purposes, Internat. Atomic Energy Agency, 2001.

[10] C. Eisenhauer, J. Hunt, R. Schwartz, Calibration techniques for neutron personal dosimetry, Radiat. Prot. Dosim. 10 (1–4) (1985) 43–57.

[11] M. Hakim, I. Zahir, S. Tassadit, A. Malika, MCNP5 evaluation of a response matrix of a Bonner sphere spectrometer with a high efficiency 6 LiI (Eu) detector from 0.01 eV to 20 MeV neutrons, J. Radioanal. Nucl. Chem. 284 (2) (2010) 253–263.

[12] P.C. Hansen, Numerical tools for analysis and solution of Fredholm integral equations of the first kind, Inverse Problems 8 (6) (1992) 849.